Applied Composite Materials (2021) 28:1829–1843
https://doi.org/10.1007/s10443-021-09928-5

Energy Absorption and Stiffness Balance in Modified and Conventional Syntactic Foams

Victor Birman[1]

Received: 19 January 2021 / Accepted: 15 June 2021 / Published online: 3 August 2021

Abstract
The paper presents the method of analysis and a comparison of the effectiveness of modified and conventional syntactic foams. The method employs the two-phase superposition approach recently developed for composite materials consisting of several concentric phases. Conventional syntactic foams consisting of spherical voids surrounded by thin glass shells embedded in the matrix are compared to modified foams with cylindrical or spheroidal voids. Modified syntactic foams analyzed in the paper include foams with cylindrical voids aligned along the applied stress or perpendicular to the stress and foams with randomly oriented cylindrical voids. It is demonstrated that while conventional syntactic foams with spherical voids absorb more energy than their modified counterparts, the stiffness of such foams is compromised due to the presence of voids to a larger degree than in modified foams. Accordingly, modified syntactic foams may appear a better compromise if a high energy absorption has to be combined with a prescribed large stiffness of the material.

Keywords Syntactic foams · Micromechanics · Energy absorption · Stiffness · Multi-phase

1 Introduction

Syntactic foams have found a wide range of applications because of their light weight, high specific strength, low coefficient of thermal expansion, low moisture absorption and other attractive properties. In conventional syntactic foams hollow or non-hollow spherical voids are surrounded with thin glass or metallic shell and embedded in the matrix. Manufacturing, design and application issues of these materials have been considered in several reviews (e.g. [1]). Micromechanics of syntactic foams with spherical coated voids has been extensively studied and explicit expressions for the bulk and shear moduli are available. In particular, the solution for the upper and lower bounds on the shear modulus and the explicit expression for the bulk modulus of elastic syntactic foams was obtained in [2, 3]. Explicit expressions for elastic constants of a syntactic foam have been derived in [4].

✉ Victor Birman
vbirman@mst.edu

[1] Department of Mechanical and Aerospace Engineering, Missouri University of Science and Technology, Rolla, MO 65409, USA

A numerical FEA methodology was employed in [5] to evaluate the properties of the interphase in syntactic foams. It has been illustrated in both numerical and experimental studies that while the tensile modulus of elasticity of a syntactic foam increases with a higher microsphere volume fraction, the tensile strength decreases [6]. Moreover, micromechanical methods have been extended to include elastic–plastic aspects of metal matrix syntactic foams [7–9], while viscoelastic response of syntactic foams was studied in [10]. Bardella et al. compared several micromechanical models of syntactic foams with spherical voids [11].

One of the attractive features of syntactic foams is a high toughness and energy absorption (e.g., [12–14]). Besides energy absorption in foams with an elastic matrix, energy absorption in metal-matrix syntactic foams has been extensively investigated [15–19]. In particular, aluminum matrix foams with iron hollow spheres were studied and showed an impressive energy absorption capacity attributed to a significant plastic yielding plateau on the stress–strain curve [17]. Advantages in the energy absorption capacity, as compared to that in conventional metal foams, was demonstrated for zinc alloy matrix, glass microballons syntactic foams in [19]. A syntactic foam with alumina cenospheres and bulk metallic matrix was manufactured and proven to combine high strength and energy absorption properties exceeding those of pure metallic glass foams [18]. A new class of metal-matrix syntactic foams was developed in [15] combining CoCrFeMnNi matrix with alumina cenospheres. These foams combine high strength attributed to the effect of ceramic shells with a high energy absorption capacity provided by the metal matrix. The behavior of syntactic foams with viscoplastic matrices subject to a high strain rate loading was considered in [20]. A comprehensive review of applications of syntactic foams is outside the scope of this paper, mentioned here are submersible vehicles, rudders of submarines, thermal insulators, propeller fillers and cores of sandwich structures. Note that a modified syntactic foam could also be manufactured with cylindrical or spheroidal inclusions, but its advantages compared to the conventional counterpart have not been thoroughly investigated.

The analysis of stiffness and energy absorption of syntactic foams relies on micromechanical modeling of concentric three-phase composites with a thin coating separating the matrix from the inclusion (Fig. 1). The unique feature attributed to syntactic foams is that the "inclusion" is often hollow possessing zero stiffness. While the solutions for spherical syntactic foams can rely on such studies as [2–6] and [21–23], other shapes of voids have not been extensively researched. In this paper we apply the recent micromechanical approach to the evaluation of the tensor of stiffness of a multi-phase composite material based on the superposition of two-phase solutions [24, 25] to compare the energy

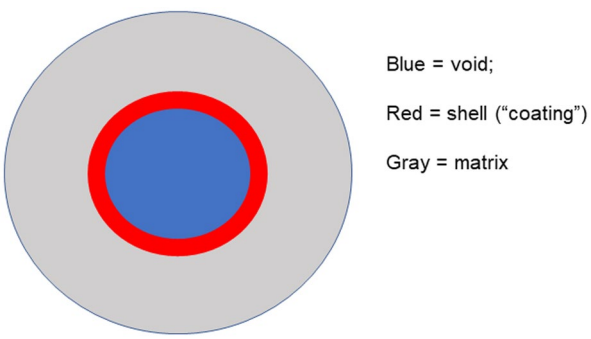

Fig. 1 Cross section of a syntactic foam. In "conventional" syntactic foams, this is a cross section of a spherical void encompassed by a thin spherical shell and the matrix. In a "modified" syntactic foam" this is a cross section of a cylindrical or spheroidal void surrounded by a thin shell and the matrix

absorption and stiffness of "conventional" syntactic foams with spherical voids to those of modified foams with cylindrical or spheroidal voids. It is demonstrated that while the energy absorption is maximum in the foams with spherical voids, these foams also possess the lowest stiffness. Accordingly, modified syntactic foams with cylindrical or spheroidal voids may present an attractive compromise increasing the energy absorption compared to that in the pristine matrix, while retaining a higher stiffness compared to their spherical void counterparts.

2 Analysis

The purpose of this paper is to analyze possible advantages and shortcomings of modified syntactic foams as compared to conventional foams with spherical voids. In all these foams hollow voids are surrounded by thin glass or metallic shells that are in turn embedded in the matrix. Here we compare the performance of foams with aligned cylindrical or spheroidal voids aligned either along of perpendicular to the applied stress direction, randomly oriented voids, and spherical voids. The basis for the comparison is the density of absorbed energy in foams subject to uniaxial or shear stress as well as the reduction in the stiffness due to the presence of voids.

In the case where inclusions or voids with a single layer of coating are embedded in the elastic matrix, the two-phase superposition method introduced by Birman [24] yields the tensor of stiffness as

$$L = L_{im}(\Omega_i, \Omega_c + \Omega_m) + L_{cm}(\Omega_i + \Omega_c, \Omega_m) - L_{cm}(\Omega_i, \Omega_c + \Omega_m) \tag{1}$$

where subscripts i, c and m refer to inclusions (or voids), coating and matrix, respectively, and Ω_j $(j = i, c, m)$ are the volumes occupied by the inclusion, coating, and matrix, respectively. Accordingly, $L_{pq}(\Omega_k, \Omega_l)$ denotes the tensor of stiffness of a two-phase composite material where phase p occupies the volume Ω_k and phase q occupies volume Ω_l.

It has been shown [24] that the present method of the evaluation of the tensor of stiffness of composites with coated inclusions provides simple and accurate solutions for fiber-reinforced materials with the fiber volume fraction up to 40% and a thin coating. In case of thicker coatings (10% volume fraction) the results were accurate if the fiber volume fraction remained below 20%. In syntactic foams the shell encompassing the void is very thin. Thus, the stiffness estimate obtained by the two-phase superposition method should be accurate with a possible exception of large void volume fractions.

Two cases of the syntactic foam are considered here, including the foams with a linear elastic matrix (e.g., polymer matrix composites) and the foams with elastic–plastic matrix (e.g., metal matrix composites).

1. Elastic Matrix

For a limited volume fraction of voids in the syntactic foam, the Mori–Tanaka method of estimating the stiffness of the composite material [26] should be accurate as follows from the previous research on fiber-reinforced and particulate composites [27]. Note that the Mori–Tanaka method for the bulk and shear moduli also represents the lower bound of the Hashin–Shtrikman if the matrix is more compliant than the inclusion and the upper bound if the matrix is stiffer, as is the case in the present problem [28], so that the results generated by this method are within the physically acceptable range.

The stiffness of two-phase uniaxially oriented spheroidal inclusions obtained employing the Mori–Tanaka approach is [29]:

$$E_{11}/E_0 = \frac{1}{1 + V_i(A_1 + 2v_0A_2)A^{-1}}$$

$$E_{22}/E_0 = \frac{1}{1 + V_i[-2v_0A_3 + (1 - v_0)A_4 + (1 + v_0)A_5A](2A)^{-1}}$$

$$G_{12}/G_0 = 1 + \frac{V_i}{\dfrac{G_0}{G_{12} - G_0} + 2(1 - V_i)S_{1212}}$$

$$G_{23}/G_0 = 1 + \frac{V_i}{G_0(G_1 - G_0)^{-1} + 2(1 - V_i)S_{2323}}$$

$$K_{23}/K_0 = \frac{(1 + v_0)(1 - 2v_0)}{1 - v_0(1 + 2v_{12}) + V_i\{2(v_{12} - v_0)A_3 + [1 - v_0](1 + 2v_{12})A_4\}A^{-1}}$$

$$v_{12} = \left[\frac{E_{11}}{E_{22}} - \frac{E_{11}}{4}(G_{23}^{-1} + K_{23}^{-1}\right]^{1/2} \tag{2}$$

where V_i is the volume fraction of the inclusion, E_{11} and E_{22} are the longitudinal and transverse moduli of elasticity, respectively, G_{12} and G_{23} are the longitudinal plane and transverse plane shear moduli, K_{23} is the plane strain bulk modulus, v_{12} is the major Poisson ratio of the composite, and v_0 is the Poisson ratio of the matrix. In Eq. (2), the stand-alone subscripts "0" and "1" refer to the matrix and inclusion properties, respectively. Both the elements of the Eshelby tensor S_{ijkl} and the coefficients A, A_n are affected by the inclusion aspect ratio. The last two Eq. (2) are coupled and can be solved by iterations.

The comparison between the results obtained by the Mori–Tanaka method to those available by the self-consistent and Halpin–Tsai methods is presented in [29]. The self-consistent and to a lesser degree the Halpin–Tsai methods yield larger longitudinal moduli at a small inclusion aspect ratio not exceeding 10. At the aspect ratio of inclusions equal to 10, the results obtained by the Halpin–Tsai and Mori–Tanaka method practically coincide, while the self-consistent method still yields higher values of the modulus. At the aspect ratio of 100 (approaching the case of continuous fibers) all three methods predict nearly identical results. Accordingly, for the aspect ratio of voids equal to or exceeding 10, the two-phase Halpin–Tsai method can be used predicting the stiffnesses as follows:

$$\begin{aligned}
E_{11}/E_0 &= \frac{1 + \xi\eta_l V_i}{1 - \eta_l V_i} \qquad \xi = 2a \quad \eta_l = \frac{E_1/E_0 - 1}{E_1/E_0 + \xi} \\
E_{22}/E_0 &= \frac{1 + \xi\eta_t V_i}{1 - \eta_t V_i} \qquad \xi = 2 \qquad \eta_t = \frac{E_1/E_0 - 1}{E_1/E_0 + \xi} \\
G_{12}/G_0 &= \frac{1 + \xi\eta_s V_i}{1 - \eta_s V_i} \qquad \xi = 1 \qquad \eta_s = \frac{G_1/G_0 - 1}{G_1/G_0 + \xi}
\end{aligned} \tag{3}$$

where α is the aspect ratio of the inclusions. Equation (3) are shown for the case where both phases of the composite material are isotropic. The major Poisson ratio can be obtained by the rule of mixtures.

In case where cylindrical voids are 2-D randomly oriented, the Tsai-Pagano method [30] can be applied to calculating the stiffness of the material that is isotropic at the macromechanical scale:

$$E = \frac{3}{8}E_{11} + \frac{5}{8}E_{22} \quad G = \frac{1}{8}E_{11} + \frac{1}{4}E_{22} \tag{4}$$

Other methods for estimating the stiffness of composite materials with 2-D and 3-D randomly oriented inclusions were developed by Nielsen and Chen [31] and by Christensen and Waals [32, 33].

Two aspects of the effectiveness of syntactic foams or modified syntactic foams for the energy absorption should be discussed. The first is the energy absorption under the prescribed load that does not cause failure of the material. As is shown in Fig. 2a, reducing the stiffness of the material results in a larger absorption of energy at the prescribed stress. However, if the requirement is preventing a catastrophic failure, the absorbed energy has to be associated with work to failure (Fig. 2b). The presence of coated voids results in local stress concentrations at the interface between the coating and the matrix as well as in the matrix adjacent to the coating. As a result, the failure stress of the foam could be reduced as compared to that in the pristine solid matrix. The opposite trends in toughness (work to failure) and strength are well documented (e.g., [34, 35]). Thus, the effectiveness of the syntactic foam in absorbing the energy at catastrophic failure has to be analyzed considering local stresses. The stress analysis in the case of uniaxially oriented spheroidal and spherical voids can be based on the solution in [36].

In this paper we concentrate on the effects of the shape and orientation of voids in syntactic foams on the reduction in the stiffness of the material and on the increase in the energy absorption. The former effect is detrimental since the voids reduce the stiffness, even though the shells (coating) may somewhat counterbalance this effect. The latter effect is positive and accordingly, designers may be interested in finding the optimum balance between the two effects. To conduct such analysis, we compare the engineering constants and the density of energy absorbed by the foam for the following materials:

- Foam with coated cylindrical voids aligned along the applied stress;
- Foam with coated voids aligned perpendicularly to the applied stress;
- Foam with randomly oriented coated voids;
- Foam with spherical coated voids.

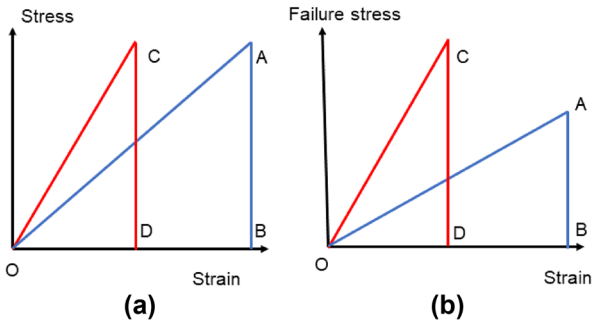

Fig. 2 (**a**) Density of absorbed energy of complaint materials represented by the area of triangle OAB is larger compared to a stiffer counterpart subject to the same stress (area of OCD), (**b**) Work to failure of a compliant material (area of OAB) is not necessarily higher than that of a stiffer material (area of OCD) since the work depends on the failure stress

Both the stiffness as well as the density of the absorbed energy are normalized with respect to those in the pristine matrix. While the stiffness is independent of the nature of load applied, the energy absorption is analyzed both for the case of a uniaxial stress as well as under the shear stress (the latter case is important if the foam is used as the core in a sandwich structure [37, 38]).

The mechanism of failure of syntactic foams has been considered in a number of experimental and numerical studies. This mechanism could be different in various classes of syntactic foams; i.e., failure in the foam with a metallic matrix differs from that in foams with epoxy matrices. In particular, Huang and Li [39] modelled the failure in foams with epoxy matrices. They found that local stresses cause the vertical splitting fracture of microspheres and the formation of microscopic cracks in the matrix. These cracks either join each other or propagate through the damaged microspheres, and finally merge into a macrocrack.

The absorbed energy density is calculated by

$$u = \int_0^{\varepsilon_i} \sigma_i d\varepsilon_i \tag{5}$$

where σ_i and ε_i are the components of the tensors of stress and strain, respectively.

In the elastic range the stress–strain relationships are linear, i.e., the tensors of stress and strain are related by

$$\boldsymbol{\sigma} = \boldsymbol{Q}\boldsymbol{\varepsilon} \tag{6}$$

where $\boldsymbol{Q}$ is the tensor of reduced stiffnesses.

The energy absorption in the case of elastic matrices is considered for a regular lifetime cycle, i.e., the foam should absorb a maximum amount of energy at the applied stresses that remain below the failure combination. Such formulation is relevant in the situations where the syntactic foam is designed to increase damping of the structure during lifetime when it is subject to loads that do not cause damage.

The energy absorption improvement factor referred to below is defined as the ratio of the absorbed energy in the unit volume cell of the syntactic foam subject to a prescribed load to the counterpart in the unit volume of the pristine matrix material subject to the same load. In the following Eqs. (7) and (8) this factor is presented for loading that does not cause damage in the material. The corresponding energy densities in the elastic range are obtained from Eqs. (5) and (6) using reduced stiffnesses calculated in terms of engineering constants of the material that are determined using Eqs. (1), (2) and (3). An extension to the case where the ductile matrix becomes plastic is outlined in the next section.

In the case of a uniaxial stress the energy absorption improvement factor of the above-mentioned types of syntactic foams for energy absorption is compared using the ratio

$$R_f = \frac{u_f'}{u^0} = \frac{Q_{11}^{(0)} - \left(Q_{12}^{(0)}\right)^2 / Q_{22}^0}{Q_{11}^{(f)} - \left(Q_{12}^{(f)}\right)^2 / Q_{22}^{(f)}} \tag{7}$$

where u_f' and u^0 are the energy densities of the foam and the pristine matrix material, respectively, and $Q_{kl}^{(j)}$ are reduced stiffnesses of the corresponding materials.

In the case of a shear stress the effectiveness of the foam is determined from

$$R_f = \frac{Q_{66}^{(0)}}{Q_{66}^{(f)}} \tag{8}$$

2. Elastic–Plastic Matrix

The approach presented above is concerned with syntactic foams with elastic matrices. However, it can be extended to ductile metal matrix composites as well. In the following, we adopt the extension of the Mori–Tanaka micromechanics [27] to the case of elastic–plastic matrices. This theory is based on averaging the strains in the matrix within the representative volume cell. Thus, the transition from the elastic to elastic–plastic response occurs throughout the entire matrix at the same stress level, rather than varying with the position vector. Within the framework of such approach the elastic–plastic response of the matrix can be modelled using the J_2 deformation theory of plasticity.

The extension of the Mori–Tanaka theory to characterize the response of composite materials with elastic–plastic or elastic-viscoplastic phases has been extensively studied (e.g., [40–42] and [43]). In particular, limiting the analysis to the small-strain J_2 deformation theory of plasticity, without unloading, the solutions have been developed for composites with elasto-plastic matrix in such papers as [44, 45]. The approach where unloading can be incorporated would be based on the so-called J_2 flow theory (e.g., Hill R. The mathematical theory of plasticity. New York: Oxford, University Press, 1950) that is not considered here.

The solution incorporating the elastic–plastic response of an isotropic matrix can be derived using the same micromechanical superposition as in the case of elastic matrices (Eq. (1)), but accounting for the physically nonlinear matrix behavior. The solution demonstrated here is based on the analysis developed by Tandon and Weng for the case of spherical inclusions [46] that was extended by Hu to fiber-reinforced composites and composites with voids [45]. The main steps of the analysis are reproduced for convenience.

The analysis of Tandon and Weng employs the assumption that the matrix material is incompressible. This implies that the bulk modulus of the matrix in the elastic stress range remains unchanged when the matrix becomes plastic. The material is assumed macroscopically isotropic meaning that the foam analyzed using the approach below has either spherical or randomly oriented coated voids.

Three superposition cases referred to in Eq. (1) involve the matrix encompassing the inclusion. The inclusion can be filled with air (first term in the right side of Eq. (1) or coating material (second and third terms in the right side of Eq. (1)). As in the previous analysis, the subscripts 0 and 1 identify the matrix and inclusion, respectively.

The plastic stress–strain relationship in the matrix material is assumed to follow the Ludwik law generalized for the case of proportional loading in terms of effective stress and effective plastic strain:

$$\overline{\sigma} = \sigma_y + h\overline{\varepsilon}_p^n \tag{9}$$

where σ_y is the yield stress, $\overline{\sigma}$ and $\overline{\varepsilon_p}$ are the effective stress and effective plastic strain, respectively, n is the work-hardening exponent and h is a material constant. The effective stress and plastic strain are determined in terms of components of deviatoric tensor of

stress and tensor of plastic strain (the components of the deviatoric stress tensor are identified by the prime):

$$\overline{\sigma} = \sqrt{\frac{3}{2}\sigma'_{ij}\sigma'_{ij}} \qquad \overline{\varepsilon}_p = \sqrt{\frac{2}{3}\overline{\varepsilon}_{pij}\overline{\varepsilon}_{pij}} \tag{10}$$

The flow rule imposed in this theory is

$$\overline{\varepsilon}_{pij} = \frac{3\overline{\varepsilon}_p\sigma'_{ij}}{2\overline{\sigma}} \tag{11}$$

Note that there are numerous matrix materials that follow the Ludwik law in the plastic range. For example, according to [45], for 6061 aluminum $h=145$ MPa, $n=0.455$, while in the example for an epoxy matrix presented in [46] $h=32.18$ MPa, $n=0.26$.

The development of the stress–strain relationships and the energy absorption analysis can be conducted as follows. Given a prescribed applied composite stress tensor $\boldsymbol{\sigma}$, the value of the secant matrix shear modulus μ_0^s has to be assumed. The secant bulk modulus is obtained by assumption that the matrix is incompressible. Accordingly, it does not differ from the bulk modulus in the elastic range, κ_0. Then the secant shear (μ^s), bulk (κ^s) and elastic (E^s) moduli as well as the Poisson ratio (ν^s) of the composite in each of three superposition cases are obtained from

$$\mu^s = \mu_0 + \frac{c_1\mu_0\left(\mu_1-\mu_0^s\right)}{\left(1-c_1\right)\beta_0^s\left(\mu_1-\mu_0^s\right)+\mu_0^s}$$

$$\kappa^s = \kappa_0 + \frac{c_1\kappa_0\left(\kappa_1-\kappa_0\right)}{\left(1-c_1\right)\alpha_0^s\left(\kappa_1-\kappa_0\right)+\kappa_0}$$

$$E^s = \frac{9\kappa^s\mu^s}{3\kappa^s+\mu^s}$$

$$\nu^s = \frac{3\kappa^s-2\mu^s}{2(3\kappa^s+\mu^s)} \tag{12}$$

where c_1 is the volume fraction of the inclusions, and

$$\alpha_0^s = \frac{1+\nu_0^s}{3\left(1-\nu_0^s\right)}$$

$$\beta_0^s = \frac{2\left(4-5\nu_0^s\right)}{15\left(1-\nu_0^s\right)} \tag{13}$$

The hydrostatic and deviatoric strains in composite can be determined from

$$\overline{\varepsilon}_{kk} = \frac{\overline{\sigma}_{kk}}{3\kappa_0} + c_1\varepsilon^*_{kk}$$

$$\overline{\varepsilon'}_{ij} = \frac{\sigma'_{ij}}{2\mu_0^s} + c_1\varepsilon_{ij}^{*\prime} \tag{14}$$

where the first terms in the right side of the equations are the average hydrostatic and deviatoric strains in the matrix, and

$$\varepsilon_{kk}^{*} = -\frac{\kappa_1 - \kappa_0}{\left[c_1 + \left(1 - c_1\right)\alpha_0^s\right]\left(\kappa_1 - \kappa_0\right) + \kappa_0}\frac{\overline{\sigma}_{kk}}{3\kappa_0}$$

$$\varepsilon_{ij}^{*\prime} = -\frac{\mu_1 - \mu_0}{\left[c_1 + \left(1 - c_1\right)\beta_0^s\right]\left(\mu_1 - \mu_0^s\right) + \mu_0^s}\frac{\sigma'_{ij}}{2\mu_0^s} \tag{15}$$

represent equivalent transformation strains [46].

The average stresses in the matrix corresponding to the prescribed values of the tensor of stress and the secant shear modulus of the matrix are

$$\sigma_{ii}^{0} = \frac{\alpha_0^s\left(\kappa_1 - \kappa_0\right) + \kappa_0}{\left[c_1 + \left(1 - c_1\right)\alpha_0^s\right]\left(\kappa_1 - \kappa_0\right) + \kappa_0}\overline{\sigma}_{ii}$$

$$\sigma_{ij}^{\prime 0} = \frac{\beta_0^s\left(\mu_1 - \mu_0\right) + \mu_0^s}{\left[c_1 + \left(1 - c_1\right)\beta_0^s\right]\left(\mu_1 - \mu_0^s\right) + \mu_0^s}\overline{\sigma}'_{ij} \tag{16}$$

The process outlined above can be applied to the evaluation of the composite tensor of stiffness and the energy absorption density in a syntactic foam. The analysis of the composite material consisting of the elastic–plastic matrix and coated voids is subdivided into three subcases:

Subcase 1: Void encompassed within the elastic–plastic matrix;

Subcase 2: Coating material occupying the volume of the coated void encompassed within the elastic–plastic matrix;

Subcase 3: Coating material occupying the volume of the void encompassed within the elastic–plastic matrix.

For each of subcases identified above, the iterative process of developing the stress–strain relationship can be developed as follows. For a prescribed applied stress tensor, the secant shear modulus in the matrix is assumed. Subsequently, composite material secant moduli and Poisson's ratio are evaluated from Eq. (12). The average stresses in the elastic–plastic matrix are found from Eq. (16) and the corresponding matrix strains are available using the first terms in the right sides of Eq. (14). The updated matrix secant modulus can now be found, compared to the previously assumed value and if necessary, employed in the new iteration.

Combining the secant stiffness tensors evaluated for each case, the secant tensor of stiffness of the syntactic foam is obtained expanding Eq. (1) that now reflects the effect of the tensor of applied stress σ:

$$\boldsymbol{L}(\boldsymbol{\sigma}) = \boldsymbol{L}_{im}\left(\boldsymbol{\sigma}, \Omega_i, \Omega_c + \Omega_m\right) + \boldsymbol{L}_{cm}\left(\boldsymbol{\sigma}, \Omega_i + \Omega_c, \Omega_m\right) - \boldsymbol{L}_{cm}\left(\boldsymbol{\sigma}, \Omega_i, \Omega_c + \Omega_m\right) \tag{17}$$

In the case of uniaxial loading, the iterative process described above is not required and the closed-form solution is available [46]. For a given plastic strain $\overline{\varepsilon_p}$, the stress in the matrix is determined by the Ludwik law (9). The secant modulus of elasticity the matrix is obtained by

$$E_0^s = \left(1/E_0 + \overline{\varepsilon_p}/(\sigma_y + h\varepsilon_p^{-n})\right)^{-1} \tag{18}$$

Other secant matrix engineering constants can be evaluated following [46]. Subsequently, the secant constants of the composite material corresponding to the prescribed plastic strain in the matrix are specified from Eq. (12).

The applied composite stress $\overline{\sigma}_{11}$ is available from the first Eq. (16). The corresponding plastic strain in the composite material is

$$\overline{\varepsilon}_{11} = \frac{\overline{\sigma}_{11}}{\left(1/_{E_s} - 1/_{E}\right)} \tag{19}$$

The energy absorption density for the syntactic foam is obtained using Eq. (5) and the composite stress–strain diagrams developed as shown above.

3 Numerical Examples

The results shown below are limited to the case of elastic matrices. Thus, they are relevant if the goal is to provide a sufficient energy absorption under design loading, while retaining a required stiffness of the foam.

The properties of foams analyzed below are:

Matrix (epoxy resin): Moduli of elasticity and shear are equal to 3.2 GPa, 1.23 GPa, respectively.

Glass shell (coating): Moduli of elasticity and shear are equal to 72.0 GPa and 31.3 GPa, respectively.

The volume fraction of glass shells is taken equal to 0.01, while the volume fraction of hollow voids vary from 0.1 to 0.5. The aspect ratio of cylindrical voids was kept at 10. Note that the maximum volume fraction of randomly oriented voids or fibers decreases with a smaller aspect ratio. For example, extensive research on the effect of geometry on the maximum packing density of inclusions was conducted by Torquato and his associates. In particular, extrapolating the results for prolate ellipsoids presented in [47] to the aspect ratio of 10, yields an estimate for the maximum packing fraction of about 0.45 (also suggested by Prof. S. Torquato in private correspondence). Similar estimates follow from experiments [48].

The moduli of elasticity of various foams normalized with respect to the elastic modulus of the solid matrix materials are presented in Fig. 3. All moduli exhibit a decrease as the volume fraction of voids increases. The axial stiffness of material in the direction of voids is higher than in the perpendicular direction. This is partly explained by the stiffening effect of the glass shell. It is noted that at a low void volume fraction the longitudinal stiffness of foam with aligned voids exceeds that of the pristine matrix reflecting the contribution of the glass constituent. The stiffness of the foam with randomly oriented voids is lower than that of the foam with aligned voids in the longitudinal direction but higher than the stiffness of such foam in transverse direction. The stiffness of the syntactic foam with spherical inclusions is lower than that of the counterparts with aligned or randomly oriented voids. In the case where the voids are oriented in the perpendicular direction to the load, the moduli E_{11} and E_{22} are interchanged, i.e., the stiffness in the load direction is compromised by the voids to a larger extent as compared to the foam with the voids aligned with the applied stress.

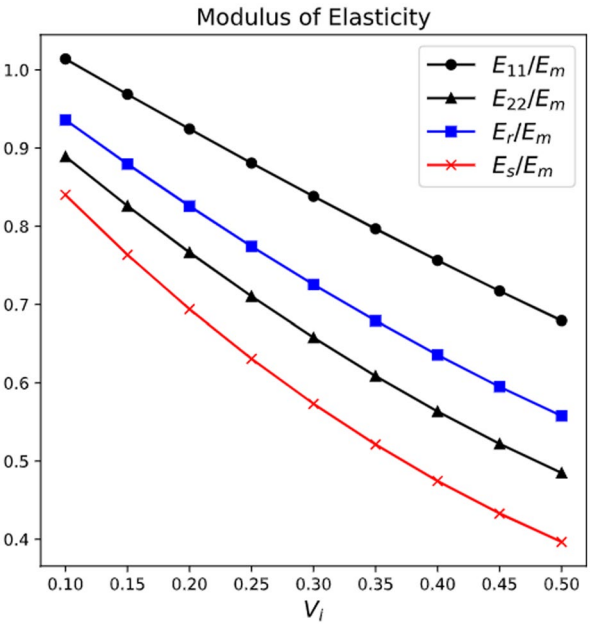

Fig. 3 Moduli of elasticity of syntactic foams normalized by the modulus of the solid matrix (E_m). E_{11} and E_{22} are the moduli in the axial and transverse directions, respectively, E_r is the modulus of the foam with randomly distributed voids, E_s is the modulus of the foam with spherical voids. Note that the maximum volume fraction of randomly packed coated voids with the aspect ratio of 10 cannot exceed the values in the range from 0.40 to 0.45 ([47], private correspondence with Prof. Torquato)

The in-plane shear stiffness of foams normalized with respect to the shear modulus of the matrix is shown in Fig. 4. Similar to the moduli of elasticity, the shear stiffness decreases with a higher void volume fraction. However, contrary to the moduli of elasticity, the shear stiffness of foams with randomly oriented voids is higher than that for the counterparts with aligned voids. The shear stiffnesses of foams with spherical and aligned

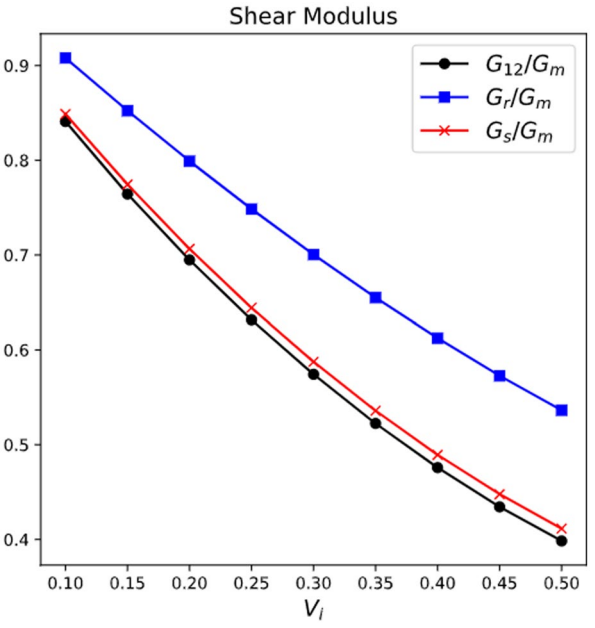

Fig. 4 Moduli of shear of syntactic foams normalized by the solid matrix shear modulus (G_m). G_{12} is the in-plane shear modulus, G_r is the shear modulus of the foam with randomly distributed voids, G_s is the modulus of the foam with spherical voids. Note that the maximum volume fraction of randomly packed coated voids with the aspect ratio of 10 cannot exceed the values in the range from 0.40 to 0.45 ([47], private correspondence with Prof. Torquato)

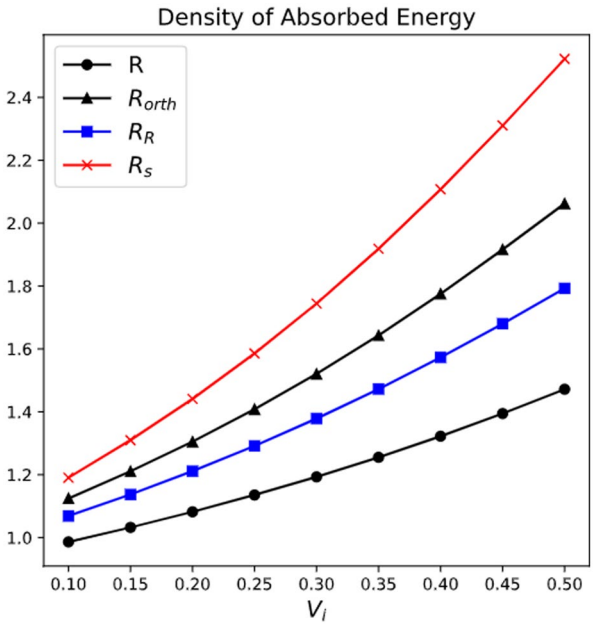

Fig. 5 Energy absorption in syntactic foams normalized by the absorption in the solid matrix. R is the ratio of absorbed energy in case where the voids are oriented along the applied stress, R_{orth} is the energy ratio for voids aligned perpendicular to the stress, R_r is the energy ratio for randomly oriented voids, R_s is the ratio of energy for spherical voids. Note that the maximum volume fraction of randomly packed coated voids with the aspect ratio of 10 cannot exceed the values in the range from 0.40 to 0.45 ([47], private correspondence with Prof. Torquato)

voids almost coincide. Note that the ratio of absorbed energy of syntactic foams to that of the pristine matrix material subject to shear loading and calculated by Eq. (8) represent an inverse of the ratio of shear stiffnesses shown in Fig. 4. Accordingly, we conclude that foams with spherical or aligned voids are more efficient as energy absorbers than foams with randomly oriented voids, but at the expense of a larger loss in the stiffness.

The ratios of the density of absorbed energy of syntactic foams to that of the solid matrix material undergoing a uniaxial stress are presented in Fig. 5. The foams with spherical voids exhibit the highest energy absorption capacity, but similar to the case of shear loading, this is achieved at the expense of a larger loss in the stiffness (compare Figs. 3 and 5. On the contrary, the foams with voids aligned in the direction of the load have the lowest energy absorption, while retaining the highest stiffness.

4 Conclusions

The paper compares relative advantages and shortcomings of several architectures of syntactic foams in terms of the stiffness and energy absorption. The analysis is conducted using the recently introduced two-phase superposition method to evaluate the stiffness of the material. The energy absorption magnification factor of the foams is analyzed under uniaxial and in-plane shear loads. The "conventional" syntactic foam with spherical voids has been shown to provide the highest energy absorption capacity under uniaxial load and nearly the same capacity with the foam with aligned voids under shear loading. However, this was achieved at the cost of the highest decrease in the stiffness. Therefore, in applications that require both the energy absorption as well as retaining a required stiffness, one of foam architectures discussed here can be considered as an alternative to changing the volume fraction of spherical voids or surrounding them shells.

Acknowledgements Discussions with Drs. Ajey Dambal and Salvatore Torquato are warmly appreciated.

Data Availability Data sharing not applicable to this article as no datasets were generated or analyzed during the current study.

References

1. Shutov F. A.: Syntactic polymer foams. Adv. Polym. Sci. 63–123 (1986)
2. Marur, P.R.: Effective elastic moduli of syntactic foams. Mater. Lett. **59**(14–15), 1954–1957 (2005). https://doi.org/10.1016/j.matlet.2005.02.034
3. Lee, K.J., Westmann, R.A.: Elastic properties of hollow-sphere-reinforced composites. J. Compos. Mater. **4**(2), 242–252 (1970). https://doi.org/10.1177/002199837000400209
4. Lanhong, D., Zhuping, H., Reri, W.: An explicit expression of the effective moduli for composite materials filled with coated inclusions. Acta Mech. Sin./Lixue Xuebao **14**(1), 37–52 (1998). https://doi.org/10.1007/bf02486829
5. Yu, M., Zhu, P., Ma, Y.: Identification of the interface properties of hollow spheres filled syntactic foams: An inverse strategy combining microstructural modeling with Kriging metamodel. Compos. Sci. Technol. **74**, 179–185 (2013). https://doi.org/10.1016/j.compscitech.2012.11.002
6. Carolan, D., Mayall, A., Dear, J. P., Fergusson, A. D.: Micromechanical modelling of syntactic foam. Compos. Part B Eng. **183**, 107701 (2020). https://doi.org/10.1016/j.compositesb.2019.107701
7. Dai, L.H., Ling, Z., Bai, Y.L.: Size-dependent inelastic behavior of particle-reinforced metal-matrix composites. Compos. Sci. Technol. **61**(8), 1057–1063 (2001). https://doi.org/10.1016/S0266-3538(00)00235-9
8. Orbulov, I. N., Szlancsik, A.: On the mechanical properties of aluminum matrix syntactic foams. Adv. Eng. Mater. Rev. **20**(5), 1700980 (2018). https://doi.org/10.1002/adem.201700980.
9. Orbulov, I. N., Szlancsik, A., Kemény, A., Kincses, D.: Compressive mechanical properties of low-cost, aluminium matrix syntactic foams. Compos. Part A Appl. Sci. Manuf. **135**, 105923 (2020). https://doi.org/10.1016/j.compositesa.2020.105923
10. Hariharan, G., Khare, D., Upadhyaya, P.: A micromechanical model to predict the viscoelastic response of syntactic foams. Mater. Today: Proc. **28**, 1200–1204 (2019). https://doi.org/10.1016/j.matpr.2020.01.216. [Online]. Available: https://www.semanticscholar.org/paper/A-micromechanical-model-to-predict-the-viscoelastic-Hariharan-Khare/4be4a40c6c53f371002c80a03efcdf359a70d92b
11. Bardella, L., Sfreddo, A., Ventura, C., Porfiri, M., Gupta, N.: A critical evaluation of micromechanical models for syntactic foams. Mech. Mater. **50**, 53–69 (2012). https://doi.org/10.1016/j.mechmat.2012.02.008
12. Pham, T.M., Chen, W., Kingston, J., Hao, H.: Impact response and energy absorption of single phase syntactic foam. Compos. Part B Eng. **150**, 226–233 (2018). https://doi.org/10.1016/j.compositesb.2018.05.057
13. Sahu, S., Ansari, M.Z., Mondal, D.P., Cho, C.: Quasi-static compressive behaviour of aluminium cenosphere syntactic foams. Mater. Sci. Technol. **35**(7), 856–864 (2019). https://doi.org/10.1080/02670836.2019.1593670
14. Zhang, B., Lin, Y., Li, S., Zhai, D., Wu, G.: Quasi-static and high strain rates compressive behavior of aluminum matrix syntactic foams. Compos. Part B: Eng. **98**, 288–296 (2016). https://doi.org/10.1016/j.compositesb.2016.05.034
15. Meng, J., Liu, T. W., Wang, H. Y., Dai, L. H.: Ultra-high energy absorption high-entropy alloy syntactic foam. Compos. Part B Eng. **2007**, 108563 (2021). https://doi.org/10.1016/j.compositesb.2020.108563
16. Wei, X., Chen, J.H., Dai, L.H.: Energy absorption mechanism of open-cell Zr-based bulk metallic glass foam. Scr. Mater. **66**(10), 721–724 (2012). https://doi.org/10.1016/j.scriptamat.2012.01.039
17. Szlancsik, A., Katona, B., Bobor, K., Májlinger, K., Orbulov, I.N.: Compressive behaviour of aluminium matrix syntactic foams reinforced by iron hollow spheres. Mater. Des. **83**, 230–237 (2015). https://doi.org/10.1016/j.matdes.2015.06.011
18. Lin, H., Wang, H.Y., Lu, C., Dai, L.H.: A metallic glass syntactic foam with enhanced energy absorption performance. Scr. Mater. **119**, 47–50 (2016). https://doi.org/10.1016/j.scriptamat.2016.03.034
19. Pan, L., et al.: Zn-matrix syntactic foams: Effect of heat treatment on microstructure and compressive properties. Mater. Sci. Eng. A **731**, 413–422 (2018). https://doi.org/10.1016/j.msea.2018.06.072
20. Shams, A., Panteghini, A., Bardella, L., Porfiri, M.: A micromechanical model to study failure of polymer-glass syntactic foams at high strain rates. Comput. Mater. Sci. **135**, 189–204 (2017). https://doi.org/10.1016/j.commatsci.2017.04.007
21. Benveniste, Y., Dvorak, G.J., Chen, T.: Stress fields in composites with coated inclusions. Mech. Mater. **7**(4), 305–317 (1989). https://doi.org/10.1016/0167-6636(89)90021-5

22. Luo, H. A. Weng, G. J.: On eshelby's s-tensor in a three-phase cylindrically concentric solid, and the elastic moduli of fiber-reinforced composites. Mech. Mater. **8**(2), 77–88 (1989). https://doi.org/10.1016/0167-6636(89)90008-2
23. Wang, Z., Oelkers, R.J., Lee, K.C., Fisher, F.T.: Annular Coated Inclusion model and applications for polymer nanocomposites – Part I: Spherical inclusions. Mech. Mater. **101**, 170–184 (2016). https://doi.org/10.1016/j.mechmat.2016.07.004
24. Birman, V.: Stiffness of three-phase concentric composite solids. Glob. J. Eng. Sci. **6** (2020)
25. Birman, V.: Stiffness of composites with coated inclusions. Compos. Commun. 100604 (2020)
26. Benveniste, Y.: A new approach to the application of Mori-Tanaka's theory in composite materials. Mech. Mater. **6**(2), 147–157 (1987)
27. Yin, H. M. Sun, L. Z. Paulino G. H.: Micromechanics-based elastic model for functionally graded materials with particle interactions. Acta Mater. **52**(12), 3535–3543 (2004). https://doi.org/10.1016/j.actamat.2004.04.007
28. Luo, H.A., Weng, G.J.: On Eshelby's inclusion problem in a three-phase spherically concentric solid, and a modification of Mori-Tanaka's method. Mech. Mater. **6**(4), 347–361 (1987). https://doi.org/10.1016/0167-6636(87)90032-9
29. Tandon, G.P., Weng, G.J.: The effect of aspect ratio of inclusions on the elastic properties of unidirectionally aligned composites. Polym. Compos. **5**(4), 327–333 (1984). https://doi.org/10.1002/pc.750050413
30. Tsai, S. W., Pagano N. J.: Invariant properties of composite materials. Air Force Materials Lab Wright-Patterson AFB, Ohio (1968)
31. Nielsen, L. E., Chen, P.E.: Young modulus of composites with randomly oriented fibers. J. Mater. 352–358 (1968)
32. Christensen, R.M., Waals, F.M.: Effective stiffness of randomly oriented fibre composites. J. Compos. Mater. **6**(4), 518–532 (1972). https://doi.org/10.1177/002199837200600407
33. Christensen, R.M.: Asymptotic modulus results for composites containing randomly oriented fibers. Int. J. Solids Struct. **12**(7), 537–544 (1976)
34. Gibson, L.J., Ashby, M.F.: Cellular solids, structure and properties, 2nd edn. Cambridge University Press, Cambridge (1997)
35. Hu, Y., Birman, V., Deymier-Black, A., Schwartz, A.G., Thomopoulos, S., Genin, G.M.: Stochastic interdigitation as a toughening mechanism at the interface between tendon and bone. Biophys. J . **108**(2), 431–437 (2015)
36. Tandon, G. P. Weng, G.J.: Stress distribution in and around spheroidal inclusions and voids at finite concentrations. J. Appl. Mech. **53**, 511–518 (1986)
37. Paul, D., Velmurugan, R., Gupta, N.K.: Experimental and analytical studies of syntactic foam core composites for impact loading. Int. J. Crashworthiness (2020). https://doi.org/10.1080/13588265.2020.1797346
38. Omar, M. Y., Xiang, C., Gupta, N., Strbik III, O. M., Cho, K.: Syntactic foam core metal matrix sandwich composite: Compressive properties and strain rate effects. Mat. Sci. Eng. A **643**, 156–168 (2015). https://doi.org/10.1016/j.msea.2015.07.033
39. Huang, R., Li, P.: Elastic behaviour and failure mechanism in epoxy syntactic foams: The effect of glass microballoon volume fractions. Compos. Part B Eng. **78**, 401–408 (2015). https://doi.org/10.1016/j.compositesb.2015.04.002
40. Pettermann, H.E., Plankensteiner, A.F., Böhm, H.J., Rammerstorfer, F.G.: Thermo-elasto-plastic constitutive law for inhomogeneous materials based on an incremental Mori-Tanaka approach. Comput. Struct. **71**(2), 197–214 (1999). https://doi.org/10.1016/S0045-7949(98)00208-9
41. Doghri, I., Ouaar, A.: Homogenization of two-phase elasto-plastic composite materials and structures: Study of tangent operators, cyclic plasticity and numerical algorithms. Int. J. Solids Struct. **40**(7), 1681–1712 (2003). https://doi.org/10.1016/S0020-7683(03)00013-1
42. Czarnota, C., Kowalczyk-Gajewska, K., Salahouelhadj, A., Martiny, M., Mercier, S.: Modeling of the cyclic behavior of elastic-viscoplastic composites by the additive tangent Mori-Tanaka approach and validation by finite element calculations. Int. J. Solids Struct. **56**, 96–117 (2015). https://doi.org/10.1016/j.ijsolstr.2014.12.002
43. Sadowski, P., Kowalczyk-Gajewska, K., Stupkiewicz, S.: Consistent treatment and automation of the incremental Mori-Tanaka scheme for elasto-plastic composites. Comput. Mech. **60**(3), 493–511 (2017). https://doi.org/10.1007/s00466-017-1418-z
44. Qiu, Y.P., Weng, G.J.: A theory of plasticity for porous materials and particle-reinforced composites. J. Appl. Mech. T. ASME **59**(2), 261–268 (1992). https://doi.org/10.1115/1.2899515
45. Hu, G.: A method of plasticity for general aligned spheroidal void or fiber-reinforced composites. Int. J. Plast. **12**(4), 439–449 (1996). https://doi.org/10.1016/S0749-6419(96)00015-0

46. Tandon, G.P., Weng, G.J.: A theory of particle-reinforced plasticity. J. Appl. Mech. T. ASME **55**(1), 126–135 (1988). https://doi.org/10.1115/1.3173618
47. Donev, A., et al.: Improving the density of jammed disordered packings using ellipsoids. Science **303**(5660), 990–993 (2004). https://doi.org/10.1126/science.1093010
48. Freeman, J. O., Peterson, S., Cao, C., Wang, Y., Franklin, S. V., Weeks, E. R.: Random packing of rods in small containers. Granul. Matter **21**(4), 84 (2019). https://doi.org/10.1007/s10035-019-0939-x